

Design of coreless PCB transformers for power and signal isolation in a modular ADC system for power quality data acquisition

Michael T. Carpenter and Mark A. H. Broadmeadow

School of Electrical Engineering and Computer Science

Queensland University of Technology

Brisbane, Australia

Email: michael.carpenter@student.qut.edu.au

Abstract—Available industrial energy meters offer high accuracy and reliability, but are typically expensive and low-bandwidth, making them poorly suited to multi-sensor data acquisition schemes and power quality analysis. An alternative measurement system is proposed in this paper that is highly modular, extensible and compact. To minimise cost, the device makes use of planar coreless PCB transformers to provide galvanic isolation for both power and data. Samples from multiple acquisition devices may be concentrated by a central processor before integration with existing host control systems. This paper focusses on the practical design and implementation of planar coreless PCB transformers to facilitate the module’s isolated power, clock and data signal transfer. Calculations necessary to design coreless PCB transformers, and circuits designed for the transformer’s practical application in the measurement module are presented. The designed transformer and each application circuit have been experimentally verified, with test data and conclusions made applicable to coreless PCB transformers in general.

I. INTRODUCTION

Industrial energy users are currently limited to expensive and low-bandwidth energy usage data collection devices. Although such metering devices are well suited to high-accuracy, high-energy systems, they are poorly suited to modular, multi-sensor data collection schemes and power quality analysis. To facilitate industrial process refinement, fault detection, energy usage and power quality analysis, an isolated, low-cost, high-bandwidth data acquisition module (herein referred to as a DAQM) is proposed. Data from the network of distributed measurement modules will be concentrated by a central processor (such as an FPGA), with a microcontroller facilitating the data logging and integration into existing control systems and computer consoles.

Considerable work has been published on the use of planar coreless PCB transformers in isolated gate drive circuits [1]–[4]. Although wireless charging systems for consumer electronics use a very similar concept, coreless PCB transformers have not seen significant use as a power and signal transfer device within commercial electronics. Since a coreless PCB transformer’s only cost is the PCB area it consumes, they are well suited for low-cost applications, and the use of standard PCB manufacturing processes makes their construction predictable and repeatable.

This paper focuses primarily on the practical application

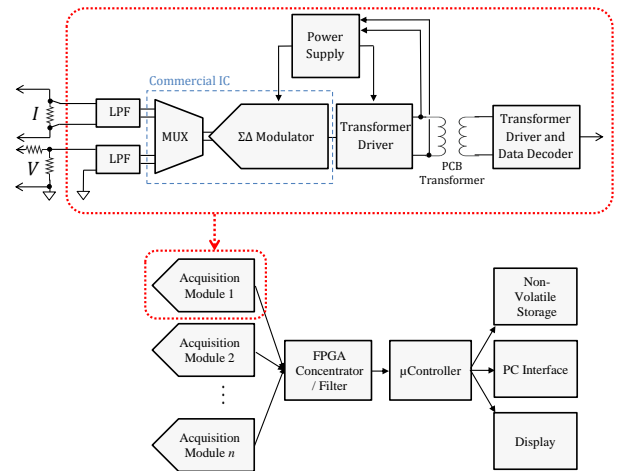


Fig. 1. Modular isolated power measurement system.

of planar coreless PCB transformers as used for the DAQM’s isolated power, clock and data signal transfer. Calculations necessary to design the coreless PCB transformers are presented, and practical circuits designed for the DAQM application, but applicable to coreless PCB transformers in general, are included. The experimental validation section demonstrates the viability of the use of coreless PCB transformers (and associated circuitry) in the DAQM application.

II. PROPOSED MODULAR DATA ACQUISITION SYSTEM

The complete data acquisition system (figure 1) is comprised of several data acquisition modules (DAQMs), a data concentrator and filter FPGA, and a microcontroller attached to a PC, display and/or storage device.

The DAQM’s data conversion device is a commercial dual-input sigma-delta ($\Sigma\Delta$) modulator IC, with appropriate external signal conditioning to allow voltage measurement via a resistor divider, and current measurement via a shunt or current transformer (CT). This paper will refer to the data conversion side of the DAQM as the “secondary” side. The primary side of the DAQM consists of the coreless PCB transformer driver and data recovery circuitry. Isolated secondary-side power and the modulator’s external clock signal is provided by a single planar coreless PCB transformer. This is teamed with a smaller,

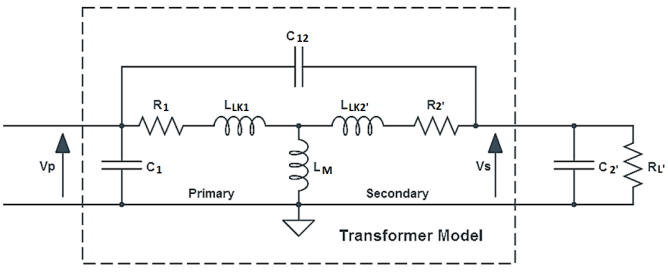


Fig. 2. High-frequency transformer model [1].

higher frequency coreless PCB transformer used to transfer measurement data from the sigma-delta modulator back to the host. For the selected sigma-delta modulator, the clock frequency will be approximately 8MHz, resulting in a data output rate of $f_{clock}/4$ (voltage and current multiplexed on one Manchester-encoded data stream) with a maximum input sampling rate of $f_{clock}/12$.

III. PLANAR CORELESS PCB TRANSFORMERS

The fundamental design of a planar coreless PCB transformer involves two planar copper spirals – one etched onto either side of a regular two (or more) layer PCB. The two windings are thus separated by the PCB’s core (or prepreg), whose material properties and thickness determine, to some extent, the transformer’s performance and isolation voltage. The transformer’s primary winding is then driven at high frequency, usually in the range of 2MHz to 20MHz in order to achieve either the maximum [input] impedance frequency (MIF; for low power systems) or the maximum efficiency frequency (MEF; for high power systems) [1]–[4]. [1] has demonstrated that an external secondary load capacitor, on the order of 100pF to 1nF, plays a significant role in the determination of the transformer’s resonant frequency. In conventional coreless PCB transformer applications, the output voltage is then rectified and filtered, and efficiencies exceeding 90%, with a power density of up to 24W/cm² have been demonstrated [1].

A two-winding coreless PCB transformer may be described using the high-frequency transformer model in figure 2 [1], where:

- R_1 Primary winding resistance;
- R'_2 Secondary winding resistance, referred to primary;
- R'_L Load resistance, referred to primary;
- L_{LK1} Primary leakage inductance;
- L'_{LK2} Secondary leakage inductance, referred to primary;
- L_M Mutual inductance;
- L_p Primary self-inductance, equal to $L_M + L_{LK1}$;
- L_s Secondary self-inductance, equal to $L_M + L_{LK2}$;
- C_{12} Primary-to-secondary winding capacitance;
- C_1 Sum of primary winding capacitance and primary driver output capacitance;
- C'_2 Sum of secondary winding capacitance and external load capacitance, referred to primary;
- n Turns ratio;
- μ_0 Permeability of vacuum;
- a_1 Inner radius of j th circular track filament;
- a_2 Outer radius of j th circular track filament;
- h_1 Height of j th circular track filament;

- r_1 Inner radius of j th circular track filament;
- r_2 Outer radius of j th circular track filament;
- h_2 Height of j th circular track filament;
- z Separation distance between the circular tracks;
- $J_0(x)$ Bessel function of the first kind, order zero.

The self inductance of the planar winding [5] is given by

$$L_p = \sum_{j=1}^{N_p} \sum_{i=1}^{N_p} M_{ij} \quad (1)$$

$$L_s = \sum_{j=1}^{N_s} \sum_{i=1}^{N_s} M_{ij} \quad (2)$$

And thus, the mutual inductance between the two planar, multi-filament windings [5] may be represented as

$$L_M = \sum_{j=1}^{N_p} \sum_{i=1}^{N_s} M_{ij} \quad (3)$$

where the filament-to-filament mutual inductance, M_{ij} , has been reported in [5]

$$M_{ij} = \frac{\mu_0 \pi}{h_1 \ln(\frac{r_2}{r_1}) h_2 \ln(\frac{a_2}{a_1})} \int_0^\infty S(kr_2, kr_1) S(ka_2, ka_1) Q(kh_1, kh_2) e^{-k|z|} dk \quad (4)$$

where

$$S(kx, ky) = \frac{J_0(kx) - J_0(ky)}{k} \quad (5)$$

$$Q(kx, ky) = \begin{cases} \frac{2}{k^2} [\cosh k \frac{x+y}{2} - \cosh k \frac{x-y}{2}] & z > \frac{h_1+h_2}{2} \\ \frac{2}{k} \left[h + \frac{e^{-kh}-1}{k} \right] & z = 0, x = y = h \end{cases} \quad (6)$$

Note that $z = 0$ for the calculation of self-inductances. To approximate the performance of the coreless PCB transformer, [1] gives the resonant frequency as

$$f_0 = \frac{1}{2\pi\sqrt{L_{eq}C_{eq}}}; \quad (7)$$

and the s -domain voltage gain (8) and input impedance (9) as

$$\frac{V_s}{V_p} = G(s) = B = \frac{\frac{1}{X_1} + sC'_{12}Y_1}{nY}; \quad (8)$$

$$Z_{in} = \frac{1}{sC'_{12}(1-nB) + \frac{1-A}{X_1} + sC'_1}. \quad (9)$$

Although not of great concern to the DAQM application (due to the low secondary power requirements), the coreless PCB transformer’s efficiency may be calculated as [1]

$$P_{out} = \frac{|G(s)|^2 \cdot |V_p|^2}{R_L}; \quad (10)$$

$$P_{in} = |V_p|^2 \cdot \Re \left[\frac{1}{Z_{in}} \right]; \quad (11)$$

and thus,

$$\eta = \frac{|G(s)|^2}{R_L \cdot \Re \left[\frac{1}{Z_{in}} \right]} \times 100\%. \quad (12)$$

Where

$$L_{eq} = L'_{LK2} + L_{LK1} || L_M$$

$$C_{eq} = C'_2 + C'_{12}$$

$$R'_2 = n^2 R_2$$

$$L'_{LK2} = n^2 L_{LK2}$$

$$C'_1 = C_1 + \frac{n-1}{n} C_{12}$$

$$C'_2 = \frac{1}{n^2} C_2 + \frac{1-n}{n^2} C_{12}$$

$$C'_{12} = \frac{1}{n} C_{12}$$

$$X_1 = R_1 + sL_{LK1}$$

$$X_2 = R'_2 + sL'_{LK2}$$

$$Y_1 = X_2 \left[\frac{1}{X_1} + \frac{1}{sL_M} \right] + 1$$

$$Y_2 = \frac{1}{X_2} + sC'_{12} + sC'_2 + \frac{1}{n^2 R_L}$$

$$Y = -\frac{1}{X_2} + Y_1 Y_2$$

$$A = \frac{sC'_{12} + \frac{X_2}{X_1} Y_2}{Y}$$

IV. IMPLEMENTATION OF POWER AND SIGNAL ISOLATION USING PCB TRANSFORMERS

A. Power

The most basic use for a planar coreless PCB transformer is in an isolated power transfer application. Typically, this would be achieved by driving the transformer at its maximum efficiency frequency (MEF) for high power transfer applications, or, where it is desirable to minimise the quiescent power consumption of the transformer, the maximum impedance frequency (MIF). The MEF will tend to approach the MIF as the transformer's secondary load current decreases [1].

Due to the low secondary load current of the DAQM, approximately 6mA at 3.3V (20mW), the MEF of the module's coreless PCB transformer was initially assumed to be equal to the MIF. In most papers discussing planar coreless PCB transformers, the primary winding is driven in either a single-ended or bipolar manner (figure 3) with a relatively high supply voltage (12V being a popular choice for isolated gate drive circuits). The DAQM is instead designed to accommodate a single 3.3V supply, and hence, the PCB transformer was driven in a bipolar manner to achieve an effective doubling of the primary drive voltage. The primary drive circuit uses a simple relaxation oscillator for the resonant frequency generation, and the transformer's winding is driven directly by the Schmitt-trigger's high-current (170mW at 85°C or ±100mA maximum) push-pull outputs (figure 4).

On the transformer's secondary side, the output waveform may simply be rectified using a voltage-doubler rectifier topology 4, with a zener clamping diode to ensure the voltage regulator's maximum input voltage is not exceeded. The additional load capacitance, primarily due to the rectifier diode array D2 and coupling capacitor C4, may be estimated as the series coupling capacitor (C4) in parallel with the sum of the two diode junction capacitances in rectifier array D2. For the

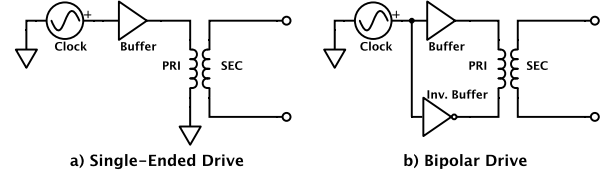


Fig. 3. Single-ended (a) and bipolar (b) transformer drive concept.

rectifier circuit shown in figure 4, the maximum additional capacitance is about 20pF, resulting in an expected resonant frequency shift of -10%.

B. Clock generation and recovery

In order to provide a clock signal of approximately 8MHz to the sigma-delta modulator, a method of transferring this clock signal (via the PCB transformer) from the DAQM's primary side to the secondary side was required. It is desirable to allow the sigma-delta modulator to be externally clocked as this allows for synchronisation in multi-module systems, thus simplifying the filtering and data concentration process.

Since the clock frequency was to remain relatively fixed, the simplest method of transferring the signal to the DAQM's isolated side was to set the coreless PCB transformer's primary drive frequency to be equal to a power-of-two multiple of the desired clock frequency. In this way, the clock signal could be extracted by rectifying, filtering and dividing the transformer's secondary voltage waveform (figure 4).

C. Data recovery

The sigma-delta modulator encodes both voltage and current information into a single Manchester-encoded bitstream at a rate equal to $f_{clock}/4$ (typically 2MHz). To transfer this data back to the primary side of the data acquisition module, a second coreless PCB transformer was used. Since the data signal is not periodic in the way that a clock signal is, it was necessary to configure the data transformer for a very high resonant frequency, thus ensuring that only the high-frequency square wave transitions were sent over the coil. To achieve this, the equations in Section III imply that either the number of primary and secondary turns (and thus the primary and secondary winding outer diameter) should be decreased, and/or the external load capacitor may be reduced or removed.

Figure 5 shows the signal transformer and data recovery circuit. On the coreless PCB transformer's secondary side, the data output of the modulator is capacitively coupled into the signal transformer, which is driven in a single-ended configuration. On the primary side, the low-amplitude (50mV to 500mV may be expected) positive- and negative-going spikes, which represent the rising and falling edges of the data signal respectively, are first amplified by a bipolar junction transistor (BJT, Q1). The amplifier's output is then coupled into two more BJTs with necessary biasing to allow the discrimination of the positive- and negative-going transitions (Q2 and Q3 respectively). The output of each of the 'edge transition detectors' is then fed into a set/reset latch constructed from a dual Schmitt-input NAND array to complete the decoding circuit. As an added benefit, the outputs of the two NAND gates are

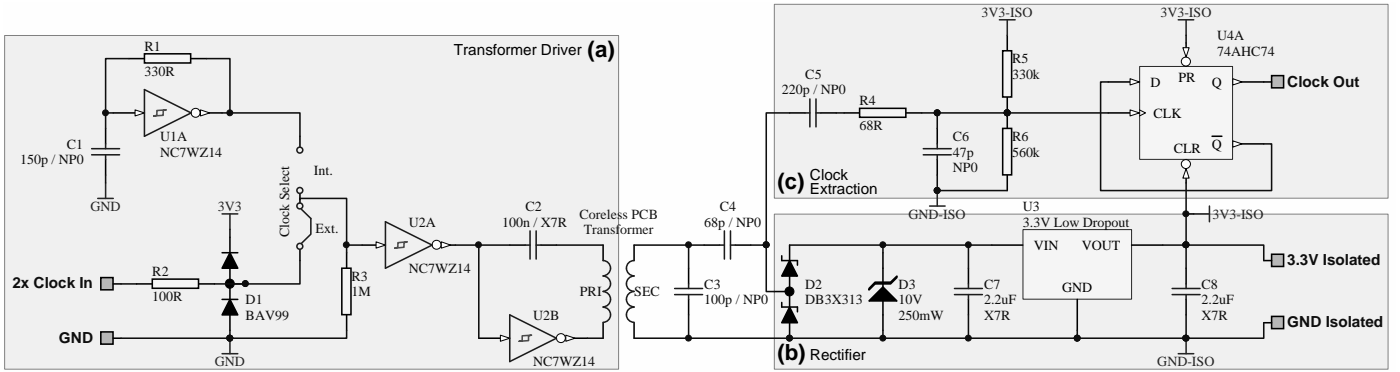


Fig. 4. Coreless PCB transformer driver (a) with power rectifier (b) and clock extraction circuitry (c) highlighted.

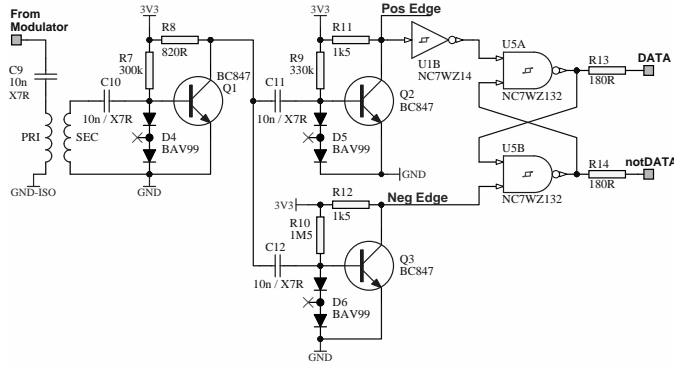


Fig. 5. Signal transformer and isolated data recovery circuit.



Fig. 6. Photograph of an initial unpopulated DAQM prototype with single 11-turn transformer.

complementary, allowing for differential signal driving back to the concentrator FPGA (which may be located some distance away).

V. EXPERIMENTAL VALIDATION

To validate the use of planar coreless PCB transformers in the data acquisition module design, a test PCB transformer was manufactured on a standard two-layer, 1.6mm PCB (figure 6). The test transformer had 11 turns with identical primary and secondary windings, a track and spacing width equal to 254 μ m (10 mil), a 100pF external load capacitor (C3 in figure 4) and a 500 Ω load resistor. With an outer diameter of 14mm and inner diameter of 2.8mm, the transformer's calculated and measured inductive parameters (200kHz test frequency) are shown in table I.

TABLE I. CALCULATED AND MEASURED EQUIVALENT CIRCUIT PARAMETERS FOR THE DESIGNED CORELESS PCB TRANSFORMER.

	Calculated	Measured	Error (%)
L_p	890.6nH	930nH	4.5%
L_{LK1}	418.5nH	465nH	10%
L_s	890.6nH	930nH	4.5%
L_{LK2}	418.5nH	465nH	10%
L_M	472.1nH	465nH	-1.5%

Figure 7 shows the test transformer's calculated and measured input impedance and voltage gain versus frequency, where only the secondary-side load resistor of 500 Ω is fitted (that is, no rectifier or clock decoder). The plots show a MEF (9dB voltage gain) at 18MHz and a MIF (142 Ω input impedance) at about 14.5MHz (measured values). The calculated performance curves are shown to be a good representation of the actual device performance, especially with regard to the coreless PCB transformer's voltage gain.

A. Power

With the rectifier (no regulator; 500 Ω load resistor) and clock extraction circuitry (figure 4) fitted, figure 8 shows the coreless PCB transformer's primary RMS drive current and rectifier output voltage versus frequency (at 3.3V drive voltage).

The figure shows a reduction in the maximum impedance and efficiency frequencies (14.5MHz and 18MHz to 13MHz and 15.5MHz respectively), most likely due to the additional load capacitance presented by the rectifier diodes. Whilst this frequency change can be predicted (as discussed prior) and accounted for by altering the load capacitor (C3 in figure 4), in this case, the desired drive frequency is 16MHz and thus adjustment was not necessary.

The experimental data also demonstrate the effectiveness of driving the transformer in a bipolar manner, which has resulted in an output voltage approximately 1.6 times the 3.3V primary supply voltage, thus increasing the usable voltage range of the data acquisition module and simplifying the secondary voltage supply circuitry. Additionally, the wide frequency range for which the output voltage is adequate for 3.3V regulation, may allow the transformer to be driven at a compromise frequency between the MIF and MEF in an effort to reduce primary drive current.

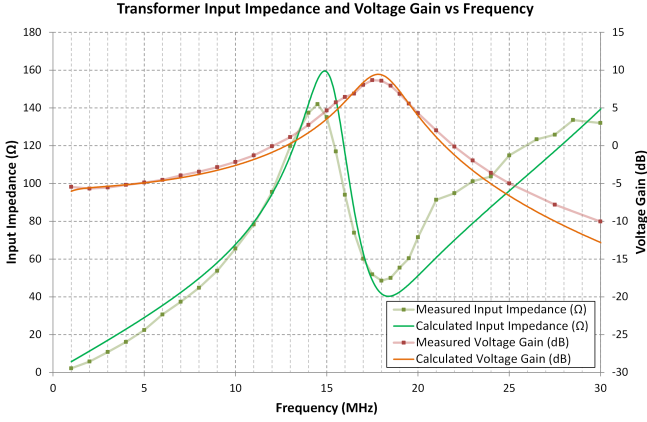


Fig. 7. Test transformer's input impedance and voltage gain versus drive frequency.

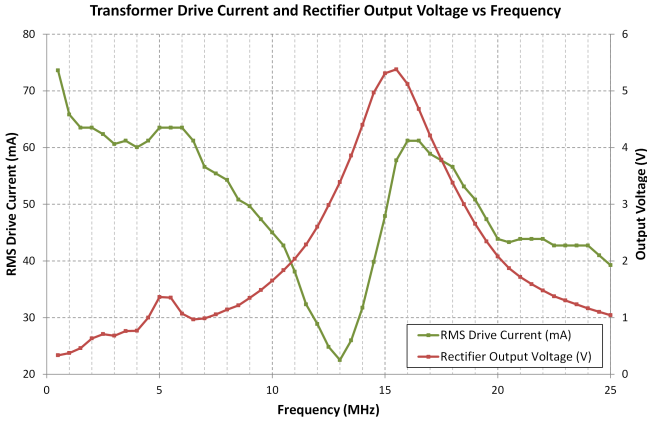


Fig. 8. Input impedance and output voltage versus frequency at 3.3V.

Figure 9 shows the coreless PCB test transformer's secondary rectified output power and voltage versus load current. It shows a maximum power point of 47mW, and that for a minimum pre-regulator voltage of 3.5V, the load current may be up to 11mA (about 40mW) – twice the expected power required by the DAQM's secondary circuitry.

As a compromise between the MIF (13MHz) and MEF (15.5MHz), the test transformer drive frequency was adjusted to 14MHz (figure 9). This data shows improved load regulation and a shift in the maximum power point toward greater load currents, as well as a slight reduction in maximum power (approximately 40mW versus 47mW). This suggests that transformer operation at a MIF-MEF compromise frequency (rather than at the MEF exactly) can have benefits for applications with relatively substantial secondary loads where the primary is driven by a current-limited source (such as the Schmitt trigger direct-drive circuit used in the DAQM design).

B. Clock generation and recovery

Since the sigma-delta modulator's clock is derived from the drive frequency of the primary winding, it is simplest for the primary drive frequency to be an exact power-of-two multiple of the desired modulator frequency, such that a series of D flip-flops may divide the signal down to the desired clock. Since the

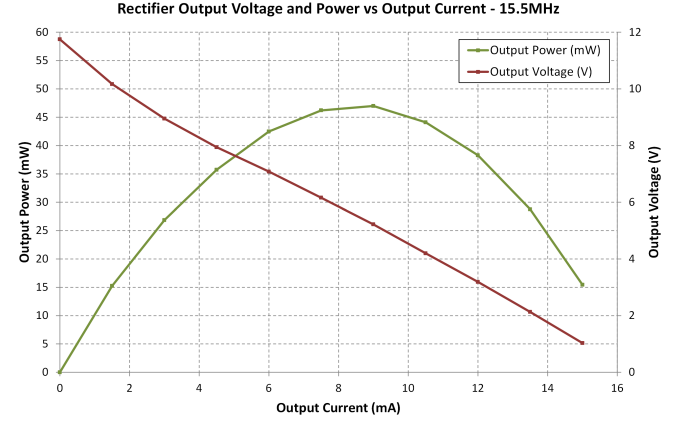


Fig. 9. Secondary output voltage and power versus load current at MEF (15.5MHz).

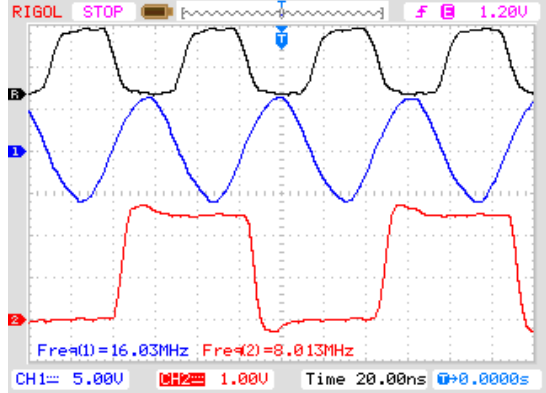


Fig. 10. 16MHz input clock signal (Reference, black [top]); secondary output voltage (Ch. 1, blue [middle]); 8MHz extracted clock signal (Ch. 2, red [bottom]).

test coreless PCB transformer has been designed for a 16MHz resonant frequency (with prior figures showing this to be a good operating point in practice), a single flip-flop was used to extract the 8MHz frequency. Figure 10 shows the 16MHz clock signal (Reference, black), secondary output voltage (Ch. 1, blue) and extracted clock signal (Ch. 2, red).

The divide-by-two clock extraction method appears effective, even with a varying secondary load, and further testing showed the simple circuit was able to accurately output a 50%-duty clock signal over the transformer drive frequency range of 11MHz to 16MHz. Based on these data it is expected that a higher order division (divide by 4, for example) could be used if desired.

C. Data Recovery

To test the data recovery circuit, a second PCB transformer was obtained with physical specifications identical to the unit discussed prior. This second test transformer, however, had its load capacitor (which was 100pF in the prior unit) removed, such that its resonant frequency was much greater than the expected data frequency – a key requirement of the data transfer method. The decoding circuit was tested by driving the transformer in a single-ended configuration with a simulated data source connected via a small coupling capacitor.

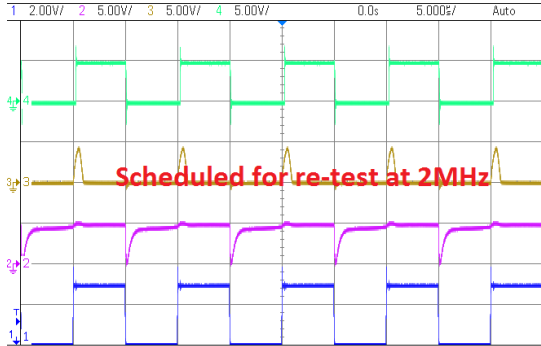


Fig. 11. Data into transformer (CH1, bottom); output of negative edge amplifier (CH2); output of positive edge amplifier (CH3); recovered data signal at output of transformer (CH4, top).

Since the data recovery circuit was capable of reliable operation with edge spikes of an amplitude as low as about 100mV, the 11-turn transformer was found to be excessive for the data signal transfer scheme. By cutting the PCB copper tracks on the primary and secondary side of the transformer, the performance of the data recovery circuit was tested for a transformer consisting of five turns and three turns respectively. The test showed that for a 3.3V square wave input, the five-turn and three-turn transformers yielded edge spikes of approximate amplitudes of 170mV and 50mV respectively.

Figure 11 shows the data recovery circuit operating at full-speed (2MHz), where Reference 1 (COLOUR) is the 3.3V, 2MHz simulated data into the 5-turn coreless PCB transformer's primary (which is on the DAQM's acquisition side); Channel 1 (COLOUR) is the voltage at the transformer's secondary (on the DAQM's host-connected side); Channel 2 is the output of the negative edge amplifier (node 'Neg Edge' in figure 5); Channel 3 is the output of the positive edge amplifier (node 'Pos Edge' in 5); and Channel 4 (COLOUR) is the recovered 2MHz data signal.

Testing has demonstrated that the data recovery circuit is effective over a range of data rates and duty cycles, and that a coreless PCB transformer with as few as four to five turns can be expected to yield reliable performance at this data rate.

VI. FUTURE WORK

The development of the coreless PCB transformer for use in the data acquisition module has yielded two key further research opportunities. With each module's coreless PCB transformer operating at 16MHz, significant electromagnetic interference (EMI), both radiated and conducted, may be expected. Whilst informal experimentation has shown that crosstalk between planarly separated modules (the intended multi-module configuration) is much less than when the modules are axially separated, a thorough analysis has not yet been performed and thus the extent and effect of inter-module interference is not yet known.

[6] demonstrates that relatively thin (0.4mm) ferrite sheets can provide effective EMI shielding – up to a shielding effectiveness of 40dB for a bare ferrite sheet, or up to 60dB for the same sheet but with copper backing. Cost analysis has shown that such a ferrite sheet may increase the module cost by 10-20%, which may represent a worthwhile inclusion.

Other methods for EMI reduction include driving the coreless PCB transformer with a sinusoidal waveform rather than the square waveform used currently, and the possibility of using a spread-spectrum driver in order to reduce the amplitude of the fundamental drive frequency.

The second area of research interest involves the transmission of the 2MHz data signal from the module's secondary side to the primary side, using the same coreless PCB transformer used to transfer the clock signal (16MHz \div 2 typical) and provide isolated secondary power. This single-transformer concept is the ultimate goal of the DAQM's coreless PCB transformer design, with the original intention being that the data signal would be load- or resonant frequency-modulated at the secondary, which could be detected by monitoring the transformer's primary-side drive current. Such disturbance detection is performed in commercial RFID systems, where the receiver modulates its antenna's resonant frequency to allow the transmitter to identify the receiving device [7].

VII. CONCLUSION

The use of planar coreless PCB transformers has received some interest due to the advent of wireless inductive charging systems; however, such transformers have not seen significant use as a power and signal transfer device in commercial electronics. This paper presented the concept of a isolated, low-cost, modular data acquisition module designed for use in a distributed multi-sensor, single-host environment. Specifically, planar coreless PCB transformers were introduced and typical design processes and calculations were presented. The paper experimentally verified the viability of the use of the coreless transformers for the module's isolated power, clock and data signals. The experimental data presented is considered to be typical of a two-winding coreless PCB transformer, and the calculations and models may be used to represent any such coreless PCB transformer design.

REFERENCES

- [1] S. C. Tang, S. Y. Hui, and H. S. Chung, "Coreless planar printed-circuit-board (PCB) transformers - A fundamental concept for singal and energy transfer," in *Power Electronics, IEEE Transactions on*, vol. 15, no. 5, September 2000, pp. 931–941.
- [2] ——, "A naturally soft-switched high-frequency gate drive circuit for power MOSFETs/IGBTs," in *Power Electronics and Drive Systems, IEEE International Conference on*, July 1999, pp. 246–252.
- [3] ——, "Optimal operation of coreless PCB transformer-isolated gate drive circuits with wide switching frequency range," in *Power Electronics, IEEE Transactions on*, vol. 14, no. 3, May 1999, pp. 506–514.
- [4] ——, "Coreless PCB-based transformers for power MOSFET/IGBT gate drive circuits," in *IEEE Power Electronics Specialist Conference*, vol. 2, 1997, pp. 1171–1176.
- [5] W. G. Hurley and M. C. Duffy, "Calculation of self and mutual impedances in planar magnetic substrates," in *Magnetics, IEEE Transactions on*, vol. 31, no. 4, July 1995, pp. 2416–2422.
- [6] Y. P. Su, X. Liu, and S. Y. Hui, "Extended theory on the inductance calculation of planar spiral windings including the effect of double-layer electromagnetic shield," in *Power Electronics, IEEE Transactions on*, vol. 23, no. 4, July 2008, pp. 2052–2061.
- [7] Y. Lee, "AN707: MCRC355/360 applications," pp. 1–3, 1999. [Online]. Available: <http://www.microchip.com/downloads/en/AppNotes/00707a.pdf>